



The Influence of Riverine Nutrients in Niche Partitioning of Phytoplankton Communities—A Contrast Between the Amazon River Plume and the Changjiang (Yangtze) River Diluted Water of the East China Sea

OPEN ACCESS

Edited by:

Christian Lonborg,
Australian Institute of Marine Science
(AIMS), Australia

Reviewed by:

María Froján,
Instituto de Investigaciones Marinas,
Vigo, Consejo Superior de
Investigaciones Científicas (CSIC),
Spain

Bingzhang Chen,
Tokyo University of Marine Science
and Technology, Japan
María Aranguren-Gassis,
University of Vigo, Spain

*Correspondence:

Helga do Rosario Gomes
helga@ldeo.columbia.edu

Specialty section:

This article was submitted to
Marine Biogeochemistry,
a section of the journal
Frontiers in Marine Science

Received: 05 April 2018

Accepted: 06 September 2018

Published: 25 September 2018

Citation:

Gomes HdR, Xu Q, Ishizaka J,
Carpenter EJ, Yager PL and Goes JI
(2018) The Influence of Riverine
Nutrients in Niche Partitioning
of Phytoplankton Communities—A
Contrast Between the Amazon River
Plume and the Changjiang (Yangtze)
River Diluted Water of the East China
Sea. *Front. Mar. Sci.* 5:343.
doi: 10.3389/fmars.2018.00343

Helga do Rosario Gomes^{1*}, Qian Xu², Joji Ishizaka², Edward J. Carpenter³,
Patricia L. Yager⁴ and Joaquim I. Goes¹

¹ Lamont Doherty Earth Observatory at Columbia, Palisades, NY, United States, ² Institute for Space-Earth Environmental Research, Nagoya University, Nagoya, Japan, ³ Estuary & Ocean Science Center, San Francisco State University, Tiburon, CA, United States, ⁴ School of Biology, Georgia Institute of Technology, Atlanta, GA, United States

Riverine nutrients act in concert with local hydrographic conditions to create distinct ecological niches for phytoplankton communities across river-ocean continuums. Here we compare two of the world's largest river-ocean systems, the Amazon River Plume (ARP) which outflows into the Western Tropical North Atlantic and the Changjiang Diluted Water (CDW) which empties into the East China Sea to show how distinctly different N:P supply ratios of their source waters, shape phytoplankton communities along the river-ocean continuum. Sampling in the relatively unpolluted surface waters of the ARP during peak river discharge revealed that phytoplankton communities along the river-ocean continuum were strongly limited by Dissolved Inorganic Nitrogen (DIN, nitrate plus nitrite) which was low or beyond detectable, while Dissolved Inorganic Phosphorous (DIP, phosphate) and Silica were not limiting. The resulting low N:P supply ratio allowed diazotrophs to co-exist with non-diazotrophs. Diatom-Diazotroph Associations (DDAs) such as *Hemiaulus hauckii*-*Richelia* proliferated, while in the oligotrophic oceanic waters, *Trichodesmium* spp. thrived. In contrast, in the CDW, anthropogenic nitrogen inputs from human pressures in the Changjiang River system has led to a system where the changing supply rate of the single nutrient (DIP) is responsible for the interannual variability seen in the phytoplankton community structure of the CDW. During years of low discharge, DIP limitation can be ameliorated by on-shelf upwelling of DIP rich Kuroshio Intermediate Waters leading to domination of diatoms and dinoflagellates. Conversely, during years of heavy discharge, the westward flowing CDW plume was severely DIP limited, probably because water column stratification dampened upwelling of subsurface waters. The consequent DIP limitation led to the proliferation of small phytoplankton such as Chlorophytes and Cyanobacteria. The absence of diazotrophs in the CDW, leads us to hypothesize that river-ocean continuums, whose source waters

are heavily impacted by anthropogenic activities and with high nitrate concentrations often substantially in excess of Redfield ratios, may not support diatoms offshore on account of DIP limitation nor diazotrophy because of excess DIN.

Keywords: Amazon River Plume, Changjiang River Diluted Water, East China Sea, resource competition, nutrient stoichiometry, phytoplankton communities, diazotrophy

INTRODUCTION

Rivers are the primary conduit transporting weathered, leached, and human-derived material from land to the oceans (Sharples et al., 2017). In addition to carbon, rivers export nitrogen, phosphorus and silica which are the key potentially limiting nutrients required for phytoplankton growth. Thus riverine nutrients can not only augment primary productivity but also contribute to regulating the long-term biological productivity of the ocean and hence ocean carbon storage (Jickells et al., 2017). Several studies show that anthropogenic disturbance of river nutrient loads and export to coastal and ocean marine systems has increased, creating a global problem affecting water quality, and biodiversity (Bouwman et al., 2005). Increasing inputs of nitrogen and phosphorus from human activity, predominantly from land-based activities, now have the potential to modify oceanic, and even global, biogeochemical systems. The total river input of nitrogen and phosphorus to the coastal seas has approximately doubled over the last few hundred years (Seitzinger et al., 2010; Beusen et al., 2016; Jickells et al., 2017). Nitrogen inputs are a consequence of urbanization, sanitation, development of sewerage systems, and lagging wastewater treatment, as well as increasing food production and associated inputs of N fertilizer, animal manure, atmospheric N deposition, and biological N fixation in agricultural systems. P has increased through the use of rock phosphate as fertilizer, detergent additives, animal feed supplements etc. (Seitzinger et al., 2010). Sharples et al. (2017) calculated that globally 75 and 80% Dissolved Inorganic Nitrogen (DIN) and Dissolved Inorganic Phosphate (DIP) respectively, reaches the open ocean although these are considered as the upper limits as estuarine processes were ignored in the study. However, there is a significant and systematic spatial variability in supply materials to the open ocean as well as the amount and kinds of nutrients supplied. Sharples et al. (2017) reported that the proportion of nutrients reaching the open ocean, from tropical and subtropical rivers tend to be the most important for nutrient delivery because the weak Coriolis force allows direct across-shelf movement of river plumes unlike in temperate and polar regions, where the Coriolis force moves freshwater flows along the shelf (Jickells et al., 2017). Hence low latitude rivers such as the Amazon, and the rivers in Southeast Asia including the Changjiang River are major sources of nutrients for the oceans or seas into which they discharge.

As nutrient loads change, so does the stoichiometry of the coastal and open ocean waters resulting mostly in increasing N:P supply ratios and consequent variations in algal communities (Glibert et al., 2014). There has been a large body of work (Anderson et al., 2002; Heisler et al., 2008; Glibert et al., 2010)

on eutrophication which report that inland and coastal waters are witnessing increased algal growth and development of high biomass blooms as well as changes in species diversity from increased riverine nutrient loads. However, only a few studies document changes in regions of the open ocean where riverine nutrients are exported and which can influence phytoplankton biodiversity and productivity.

Here we compare two widely disparate river-ocean continuums, the tropical Amazon River Plume (ARP) which outflows into the Western Tropical North Atlantic and the Changjiang Diluted Water (CDW), the plume of low salinity water from the Changjiang River which extends across East China Sea (ECS).

Comparison of the Amazon River and the Changjiang River Continuums

The magnitude of discharge ($120,000 \text{ m}^3 \text{ s}^{-1}$) from the Amazon River is unique in the global oceans; the Amazon River discharges as much freshwater as the next 8 largest rivers in the world combined (Coles et al., 2013). This tremendous volume of freshwater forms a very dynamic and extensive surface plume that protrudes well offshore into the WNTA (Figure 1a). Because the Amazon discharges at the equator and on the western boundary of the ocean, its waters are entrained in energetic boundary currents associated with the North Brazil Current, the North Equatorial Counter Current, and the coastal Guyana Current (Figure 1a; Coles et al., 2013). These currents have strong seasonal variations in response to the atmospheric Intertropical Convergence Zone (ITCZ) which is located in the southern position in winter, and northern in summer. Thus, during the winter and spring months, the plume follows the North Brazil Current along the northeastern coast of South America, carrying low salinity water to the Caribbean and in summer and fall, it retroflects to the east, entrained in the North Equatorial Counter Current (Muller-Karger et al., 1988; Coles et al., 2013; Weber et al., 2017). The discharge, introduces tremendous quantities of nutrient-rich water to the Western Tropical North Atlantic, with nutrients being mostly plant derived as it traverses for over 6000 km from the Andes in Peru to the Atlantic Ocean, and covers a watershed that includes the largest tropical rainforest in the world as well as areas of dry grassland, or savannah (Del Vecchio and Subramaniam, 2004).

The Changjiang River, the third largest in the world and the largest outflowing river in China (Yan et al., 2010) discharges into the ECS, one of the world's largest marginal seas (Figure 1b) with 70% of its area characterized by a continental shelf slope shallower than 200 m. The freshwater discharge and total

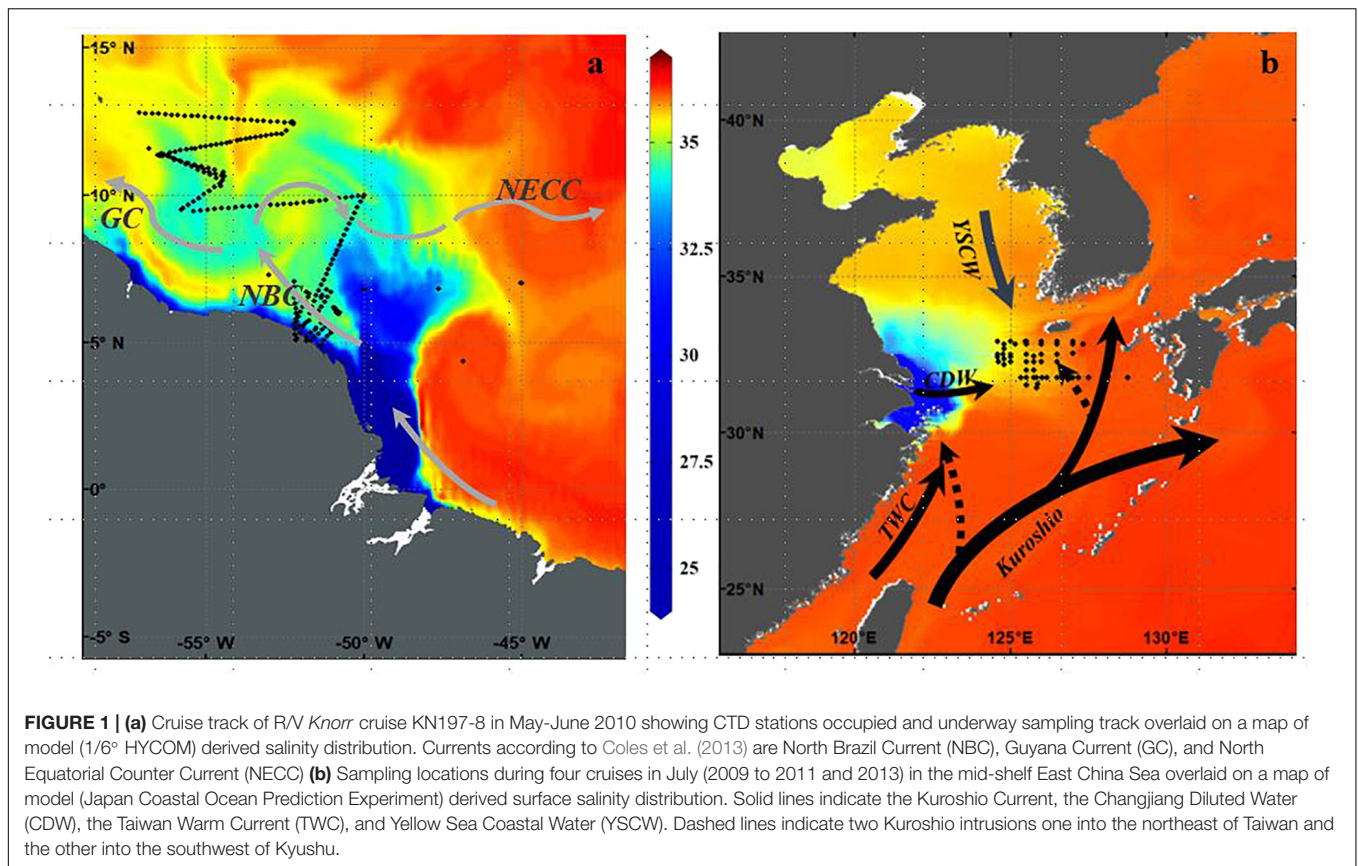


FIGURE 1 | (a) Cruise track of R/V *Knorr* cruise KN197-8 in May-June 2010 showing CTD stations occupied and underway sampling track overlaid on a map of model (1/6° HYCOM) derived salinity distribution. Currents according to Coles et al. (2013) are North Brazil Current (NBC), Guyana Current (GC), and North Equatorial Counter Current (NECC) **(b)** Sampling locations during four cruises in July (2009 to 2011 and 2013) in the mid-shelf East China Sea overlaid on a map of model (Japan Coastal Ocean Prediction Experiment) derived surface salinity distribution. Solid lines indicate the Kuroshio Current, the Changjiang Diluted Water (CDW), the Taiwan Warm Current (TWC), and Yellow Sea Coastal Water (YSCW). Dashed lines indicate two Kuroshio intrusions one into the northeast of Taiwan and the other into the southwest of Kyushu.

suspended matter from the Changjiang River spreads over the entire shelf (Sukigara et al., 2017), accounting for 90–95% of the total riverine input into the ECS (Zhang et al., 2007). Heaviest discharge is in summer in association with the monsoons with its buoyant plume, known as CDW, spreading eastward over the ECS over an area ca. $85 \times 10^3 \text{ km}^2$ (Zhang et al., 2007). In winter when discharge is lower, the northerly monsoonal winds prevail over the ECS and the Changjiang discharge is restricted to the western side of the ECS with waters moving southward and forming a narrow belt along the coast of China and toward the Taiwan Strait (Figure 1; Zhang et al., 2007). Anthropogenic activities appear to be the principal driver of the high DIN and DIP in the coastal environment of the Changjiang River (Zhang et al., 2007) with DIN inputs having increased almost 4-fold from 1970 to 2003 (Yan et al., 2010). In contrast, the Yellow Sea Coastal water flowing from the north, provides only marginal amounts of DIP and DIN (Zhang et al., 2007). High levels of nutrients from land sources brought in by the Changjiang are usually constrained to coastal and inner-shelf regions with nutrient species in surface waters gradually decreasing from eutrophic coastal to oligotrophic open shelf waters depending on the hydrographic stages of the river (Chen, 2008). Highest nitrate concentrations are found near the Changjiang estuary with DIN concentrations often exceeding $50 \mu\text{M}$ and DIP concentrations $>1 \mu\text{M}$ (Zhang et al., 2007) and in some cases N:P ratios exceeding 100 (Chen and Wang, 1999). However, large phytoplankton blooms primarily of diatoms and dinoflagellates

rapidly consume the DIP which is reduced to below $0.2 \mu\text{M}$ while DIN is still higher than $1 \mu\text{M}$ (Chen, 2008) making DIP a limiting nutrient in the shelf waters of the ECS as well as in the mid-shelf and offshore region (Wang and Wang, 2007). Off the shelf break, the northward intrusion of the nutrient-rich, sub-surface Kuroshio waters into the ECS at 50–100m depth also affects the nutrient regime of the ECS (Figure 1b). These waters can upwell in summer when winds are favorable (Zhang et al., 2007) alleviating the severe P limitation at least in the ECS shelf region (Yang et al., 2012; Yang et al., 2013; Tseng et al., 2014) Relative to shelf waters, the Kuroshio intrusion waters are high in DIN and DIP (Zhang et al., 2007) providing a much required DIP source to phytoplankton in the euphotic layer.

Compared to the Changjiang River which flows through highly industrialized regions (Beusen et al., 2016) where riverine N and P have increased tremendously, the Amazon river delivers relatively low anthropogenic inorganic nitrogen because of both less intensive catchment agriculture and dilution of nitrogen inputs by the high river flow (Jickells et al., 2017). The nitrate in this source water exists at sub-Redfield ratios, and hence is quickly drawn down by blooms of coastal diatoms that benefit from the DIP and Si-rich water (Stukel et al., 2014). This leaves a plume that extends more than 3000 km from the river mouth (Hu et al., 2004) which is nitrogen-poor but both Si and DIP rich. DIP and Si exhibit patterns that suggest near conservative mixing between high nutrient river water and oligotrophic oceanic water. Additional inputs of DIP from particle leaching both in the

estuary and offshore contribute to the low N:P ratios (DeMaster, 1996) establishing nitrogen limitation early in the life of the plume and propagated offshore (Weber et al., 2017). As the plume extends from the river mouth, it spreads as a thin cap well beyond the river mouth, leading to surface stratification that can impede nutrient inputs and strongly influence the structure of the phytoplankton communities.

While a considerable effort has been made to study the relative impacts of nutrients, physical forcing, and grazing on the phytoplankton niche communities along the Amazon river continuum (Subramaniam et al., 2008; Goes et al., 2014; Stukel et al., 2014; Conroy et al., 2016; Conroy et al., 2017; Weber et al., 2017), there is sparse information on how the CDW influences the phytoplankton community structure of the ECS. Extensive studies have focused on the nutrient contribution of the Changjiang outflow to the river-ocean continuum as well as the role of sub-surface nutrient rich Kuroshio waters (Zhang et al., 2007; Chen, 2008 and references within) in modulating the nutrient regime of the ECS while others have focused either on the phytoplankton communities of the nearshore Changjiang estuary (Li et al., 2009; Guo et al., 2014) or of the Kuroshio influenced region (Jiao et al., 2005). Our recent study (Xu et al., 2018) improves the situation by examining the phytoplankton community structure in the ECS during the summers of 3 consecutive years from 2009 to 2011 as well in 2013 clearly demonstrating the interannual variability of phytoplankton communities of the ECS associated with variations in the Changjiang River discharge and its spread eastward.

In this study we compare these two highly disparate river-ocean continuums to show that variability in the stoichiometry of their waters supports two distinct gradients of phytoplankton communities as the plumes move offshore from nutrient-rich coastal waters to offshore oligotrophic regions.

MATERIALS AND METHODS

Sampling and Hydrographic Properties ARP

In order to investigate the system of phytoplankton communities as they adapt to nutrient limitation and changing N:P ratios we undertook 3 cruises in the ARP (Coles et al., 2013; Goes et al., 2014; Stukel et al., 2014; Weber et al., 2017). This paper describes the findings of the first cruise on board the R/V *Knorr* from 22nd May to 25th June, 2010 when the discharge was at its maximum.

For a detailed description of the sampling strategies and methods, the reader is directed to Goes et al. (2014) and Weber et al. (2017). Briefly, a total of 25 stations were occupied along a cruise track (**Figure 1a**) which traversed the plume four times and extended well offshore to provide contrast with waters within the plume (Weber et al., 2017). Samples were collected with Niskin[®] bottles attached to a Conductivity-Temperature-Depth (CTD) Sea-Bird Electronics[®] Rosette from 4 depths within the euphotic zone determined from in-water profiles of photosynthetically available radiation (PAR) using a Biospherical

Instruments[®] in-water quantum scalar radiometer (Goes et al., 2014). Additionally, surface samples were collected at hourly intervals along the cruise track from the ship's uncontaminated seawater flow-through system, filtered and stored in the same manner as the hydrocast samples. While, samples were also collected from the deep chlorophyll maximum (DCM) and from below the euphotic depth, in this paper we only discuss data from surface samples and information on depth profiles is available in Goes et al. (2014). A highly refined phytoplankton structure of surface waters was obtained using microscopically determined phytoplankton species (Goes et al., 2014) while in this paper some pigment derived phytoplankton classes have also been added.

ECS

All studies were conducted on board the T/V *Nagasaki Maru* in late July of each year (**Figure 1b**). Sampling locations were confined to the ECS, in an area extending from 124.6 to 128.8°E and from 31.4 to 33.0°N. This allowed a better understanding of how phytoplankton composition in the mid-shelf ECS can be impacted by variations in the mixing of different water masses, in particular the flow and the extent of mixing of the CDW and the Kuroshio with their different nutrient contents. A more thorough and detailed description on the methods is available in Xu et al. (2018). Briefly, a CTD was used to obtain profiles of seawater Temperature (T) and Salinity (S) of the upper 80 m. Seawater samples from the surface were collected using an acid washed bucket and analyzed for pigments, and nutrients (DIN and DIP). Nutrient samples were immediately frozen in polyethylene tubes after sampling and transferred under frozen conditions to the shore laboratory for analysis using an Auto-analyzer (AACS-IV, BLTEC).

High Pressure Liquid Chromatography (HPLC) Pigment Analysis and CHEMTAX ARP

Total phytoplankton biomass was collected by gently filtering 1–2.5L surface seawater onto 47-mm GF/F filters, which were frozen in liquid nitrogen at sea and transported to shore for analysis by HPLC. Acetone extracted phytoplankton pigments were separated and characterized by methods described in Van Heukelem and Thomas (2001) and Hooker et al. (2005). Currently this method is recognized as one of the most efficient and reliable methods to analyze algal pigments (Serive et al., 2017). HPLC provided separation of almost 15 pigments including the primary pigment, Chlorophyll *a* (Chl *a*) and a suite of accessory pigments (carotenoids and chlorophylls) many of which are specific to individual phytoplankton taxa or groups (Mackey et al., 1996; Vidussi et al., 2001; Wright, 2005; Wright and Jeffrey, 2006) and can be used to categorize phytoplankton classes such as diatoms, dinoflagellates, prochlorophytes etc. This was undertaken using CHEMTAX, a free statistical software program that estimates algal class abundances from pigment markers by applying an iterative process to find the optimal ratio of biomarker pigment: Chl *a* (Mackey et al., 1996; Higgins et al., 2011) and then generates the fraction of the total Chl *a*

pool belonging to each pigment-determined group (Mackey et al., 1996). Accurate estimates necessitate that the initial or seed ratios be close to those of the phytoplankton populations that are being assessed (Latasa, 2007; Swan et al., 2016). As this constitutes the first report on pigment based phytoplankton distribution of the Amazon plume continuum we do not have pigment ratios exclusively for this region and have relied on the extensive and recently published synthesis of culture and field pigment ratios for major algal groups (Table 1; Higgins et al., 2011). These ratios have been used by Swan et al. (2016) for their global analysis and by others for select regions (Armbrecht et al., 2015; Barlow et al., 2016). However, we were also guided in our choice of ratios by microscopy data detailed in our earlier paper (Goes et al., 2014) and the extensive taxonomic report of Wood (1966) for the ARP. Another *a priori* assumption required for effective CHEMTAX analysis is that the accessory pigment-to-*chl a* ratios should be constant across the data subset under consideration i.e., the phytoplankton community must be relatively homogeneous (Swan et al., 2016). We have minimized this problem by clustering the data into subsets of pigment ratios with similarities (Dandonneau and Niang, 2007; Torrecilla et al., 2011; Wolf et al., 2014) using the statistical package PRIMER (ver. 6.1.13) on $\log(X + 1)$ transformed pigment to *Chl a* ratios from the upper 5m. Considering only linkage distances greater than 50%, our pigment ratios separated into 3 clusters (Bray Curtis similarity index) which comprised of samples from similar salinity ranges as well as coincided with the water types proposed by Goes et al. (2014) based on fluorescence data. Cluster 1 (salinity > 35) comprised mostly open ocean samples, Cluster 2 was made up of mesohaline samples in the extension of the plume (salinity 30–35), and cluster 3 were samples in the plume (salinity < 30). Each data cluster was assumed to be made up of samples of similar phytoplankton populations and CHEMTAX was run separately on each cluster.

The initial ratios or ‘true’ pigment ratios (Table 1; Higgins et al., 2011) were used to generate about 30 ‘artificial’ ratios within a certain range (S. Wright, *personal comm.*). CHEMTAX was applied to each cluster using these initial 30 matrices.

CHEMTAX quantitatively estimates the contribution of algal taxa by iteratively modifying the user-specified Pigment:Chl *a* ratios using a “steepest descent” algorithm to successively reduce the amount of unexplained pigment measured as the RMS of the residuals. The output of the matrix with the smallest RMS error was used to create 30 more matrices. However, prior to selecting this matrix, the ratios were plotted to see that they had stabilized as RMS decreased. When the RMS and the Pigment:Chl *a* ratios had stabilized, the matrices associated with the 6 best RMS were averaged. This ‘best’ matrix was then compared to the initial matrix to see if the ratios had deviated in which case the matrix was discarded. This procedure was repeated until we were confident that the RMSE was low but more importantly, that the pigment ratios had converged to within known ranges. The output (phytoplankton classes) from the 6 best RMS were averaged to provide the final phytoplankton classes for that cluster (Final Ratios in Table 1). *Prochlorococcus* sp. was quantified exclusively by its unambiguous divinyl Chlorophyll *a* (DVChl *a*) signature (Chisholm et al., 1992; Swan et al., 2016) and was not included in the CHEMTAX analysis.

ECS

Pigment analysis of samples collected in the ECS was undertaken as described in Section 2.1.2 and (Xu et al., 2018). Initial pigment ratios were from (Furuya et al., 2003) and are based on earlier pigment studies in the ECS. CHEMTAX was run as described in Section ARP. Initial and Final Ratios are shown in Xu et al. (2018). For accuracy, (see Section ARP) CHEMTAX was run on surface datasets of 2009, 2010, 2011, and 2013 separately.

Phytoplankton Taxonomy

ARP

Details of sample collection and processing for phytoplankton taxonomy are in Goes et al. (2014). Briefly, phytoplankton cells were filtered onto 8 μm pore size, 47 mm diameter Nuclepore® filters and examined under an epifluorescence microscope (Carpenter et al., 1999), and enumerated within 24 h.

TABLE 1 | Initial pigment: Chl *a* ratios entered into the CHEMTAX program are from Higgins et al. (2011), Swan et al. (2016) and Wright, S. (*personal comm.*), and Final ratios are the output after completion of CHEMTAX runs.

Phytoplankton Class	Chl c3	Chl c1	Peridinin	ButFuc	Fucoc	Prasinoc	Violax	Hex-fuco	Zea	Allox	Chl b	Chl a
INITIAL RATIOS												
<i>Prasinophytes-2</i>	0	0	0	0	0	0	0.049	0	0.032	0	0.32	1
<i>Cyptophytes</i>	0	0	0	0	0	0	0	0	0	0.38	0	1
<i>Haptophytes</i>	0.18404	0	0	0.00632	0.35	0	0	0.5	0	0	0	1
FINAL RATIOS												
Phytoplankton Class	Chl c3	Chl c1	Peridinin	ButFuc	Fucoc	Prasinoc	Violax	Hex-fuco	Zea	Allox	Chl b	Chl a
<i>Prasinophytes-2</i>	0	0	0	0	0	0.174	0.01747	0	0.01988	0	0.15524	1
<i>Cyptophytes</i>	0	0	0	0	0	0	0	0	0	0.26514	0	1
<i>Haptophytes</i>	0.28286	0	0	0.23239	0.22161	0	0	0.82225	0	0	0	1

These ratios are for analysis of pigments from the ARP while similar ratios for the ECS can be found in Xu et al. (2018). Pigment abbreviations are Chlorophyll *c3* and *c1* (Chl *c3*, *c1*), Chlorophyll *b* (Chl *b*), Chlorophyll *a* (Chl *a*), 19’butanoyloxyfucoxanthin (ButFuc), Fucoxanthin (Fucoc), Prasinocanthin (Prasinoc), Violocanthin (Violax), 19’hexanoyloxyfucoxanthin (Hex-fuco), Zeaxanthin (Zea), and Alloxanthin (Allox).

ECS

Taxonomy was solely based on pigments and no microscopy was undertaken.

RESULTS

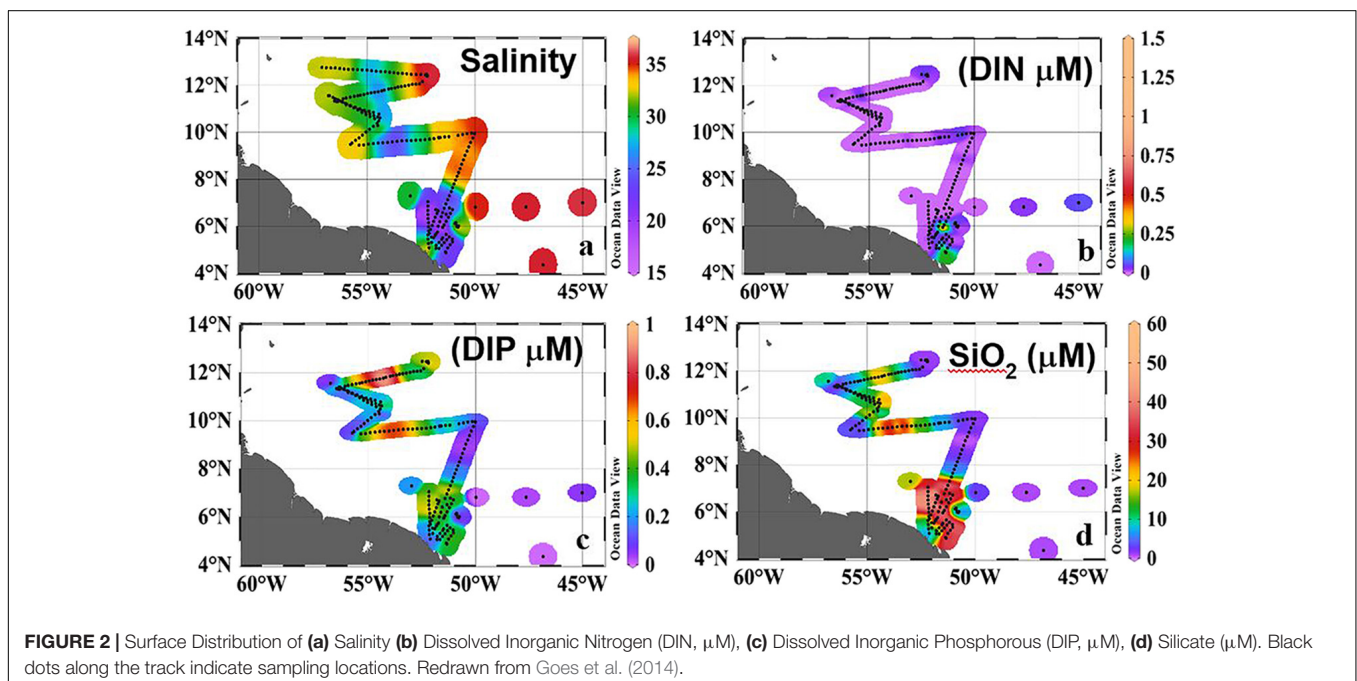
ARP

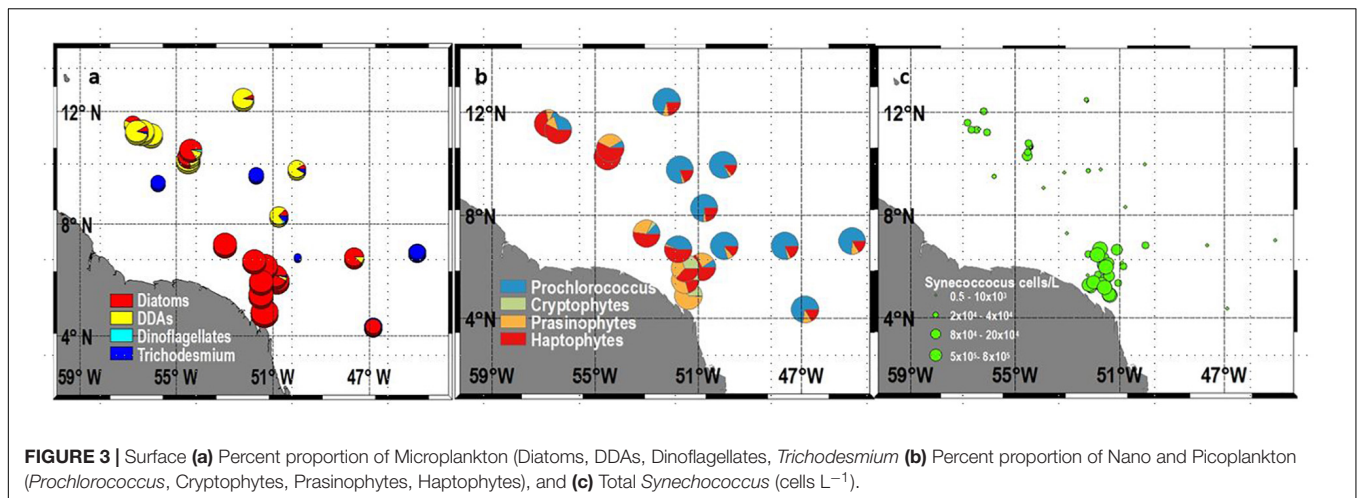
The trajectory of the ARP is clearly defined by its salinity gradient (Figures 1a, 2a) as it traveled northward in narrow coastal band, broadening and dispersing off the continental shelf at around 8°N. Salinities < 35 were evident as far north as 18°N and west of 47°W (Figure 2a). Based on high frequency fluorescence data we previously delineated three water types along the plume continuum (Goes et al., 2014), which are coincident with the salinity based demarcations of Subramaniam et al. (2008). These water types include an oceanic type of high salinity (salinity > 35), a mesohaline type with salinities from 30–35, and plume waters with salinity < 30.

The ARP clearly influenced the nutrient (DIN, DIP, and SiO₃) concentrations of the otherwise oligotrophic Western Tropical North Atlantic. DIN was almost depleted from the waters by large coastal blooms (Goes et al., 2014; Figure 2b) and concentrations ranging from 0.1–1.5 μM were found at only 9 locations, 6 of them in the plume. The highest value of 1.5 μM was at 6°N (Figure 2b) where depth profiles indicated an upward flux of the nutrient from deeper depths (see vertical profile in Figure 4e of Goes et al., 2014). In contrast, higher concentrations of DIP (Figure 2c) and SiO₃ (Figure 2d) were measured in the plume than in the surrounding waters indicating riverine influence. Although DIP distribution followed the conservative mixing line at least below 9°N, north of this, there were strong positive deviations along the axis of the plume (Goes et al., 2014; Weber

et al., 2017) which have been ascribed to the release of DIP from suspended particles and dissolved organic matter (Goes et al., 2014; Weber et al., 2017). N:P ratios of surface waters were mostly negative indicating severe nitrogen limitation. This is best illustrated using the diagnostic parameter Excess Nitrate (ExN), which measures departure from classic Redfield ratios and is calculated as $ExN = DIN - (R * DIP)$ (R = Redfield N:P ratio of 16). ExN values of < 0 indicate DIP enrichment, while $ExN > 0 \mu M$ (N:P > 16) indicates the converse (Wong et al., 1998). ExN was consistently between -17.5 and -7.5 as the plume moved northwestward indicating severe DIN limitation. Low ExN arises from a combination of rapid uptake of DIN in the plume and the addition of DIP from leaching (Fox et al., 1986). Surface SiO₃ concentrations (Figure 2d) ranged widely from 0.37 to 50 μM and mostly followed a conservative behavior as a function of salinity but with lower values in the plume and the northwestern edge of the plume because of high uptake rates by diatoms (Figure 2d).

Pigment derived phytoplankton classes and microscopically determined phytoplankton communities show the formation of niches governed by the stoichiometry of the region. A very dense and mixed bloom of diatoms comprising primarily of *Skeletonema marinoi* (*sensu lato, costatum*), *Pseudo-nitzschia* spp., *Thalassiosira alienii*, and *Chaetoceros* spp. occupied the low salinity core of the plume (Figure 3a). These blooms were fueled by riverine derived SiO₃ (Figure 2d) and cross-shore and upward flux of DIN into the surface layers. Maximum cell counts for some of the diatom species included *Pseudo-nitzschia* spp. (1.5×10^6 cells L⁻¹), *Thalassiosira* spp. (3.5×10^6 cells L⁻¹), *Guinardia flaccida* (9.0×10^4 cells L⁻¹), *Chaetoceros* spp. (3.6×10^5 cells L⁻¹), *Coscinodiscus* (3.38×10^6 cells L⁻¹), and *Odontella sinensis* (4.5×10^7 cells L⁻¹). These blooms depleted DIN from surface waters in the mesohaline and open ocean regions (Figure 2b).





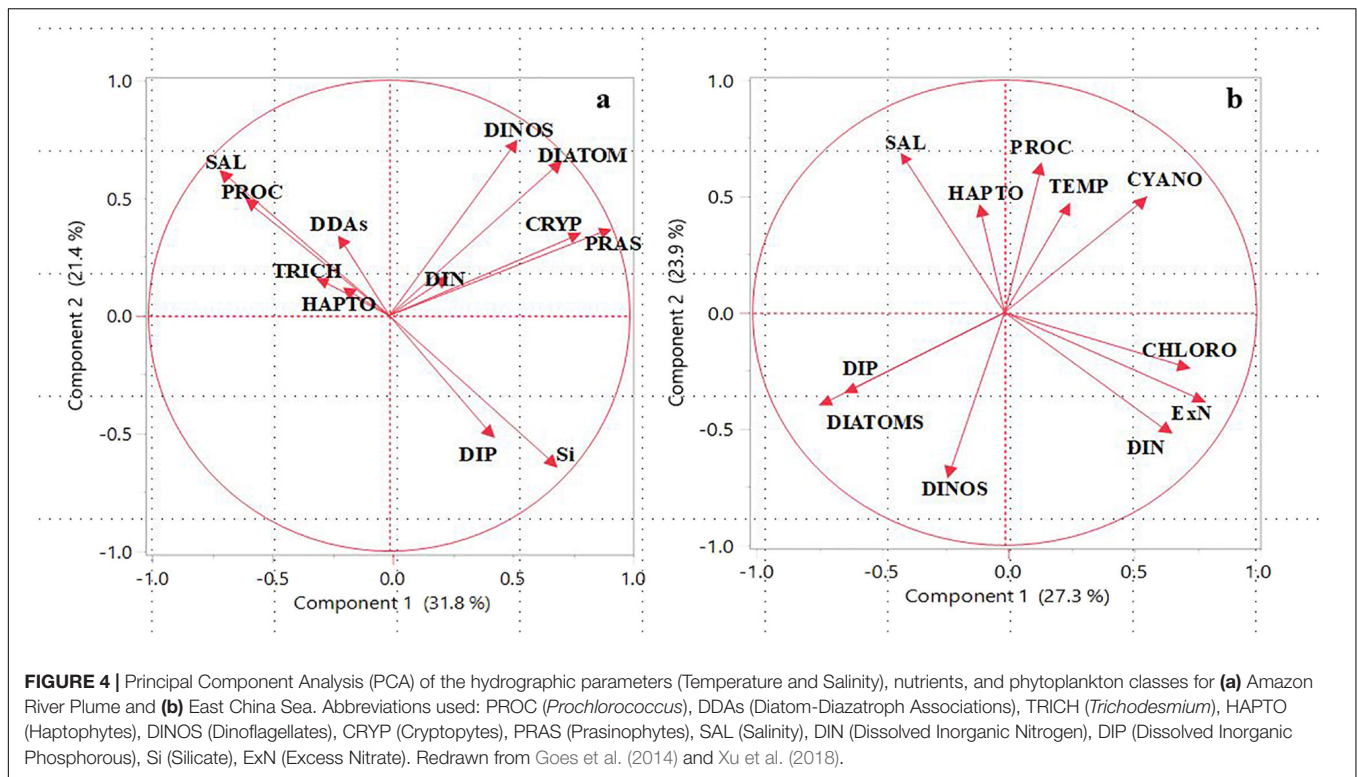
Consequently, in the mesohaline waters, the moderately high Silicate (28–33 μM) and DIP (0.5–0.9 μM) allowed a very different group of diatoms, the DDAs to emerge (Figure 3a). These symbiotic diatom-diazotrophic assemblages are capable of photosynthesizing and growing actively in the absence of DIN, because their nitrogen requirements are met via the N_2 fixing ability of their endosymbiont *Richelia intracellularis* (Foster et al., 2007; Foster et al., 2011). The dominant DDA was *Hemiaulus hauckii* with a maximum cell count of 9.7×10^5 cells L⁻¹ and high cell counts on the western side of the plume. Another DDA, *Rhizosolenia clevei* was also observed but in much smaller numbers, with maximum concentrations of about 800 cells L⁻¹. Additionally, the free living, non-symbiotic, cyanobacteria, *Trichodesmium* was also seen but more broadly distributed than the DDAs. Higher *Trichodesmium* concentrations were seen just north of the plume and in the oligotrophic waters east of the plume (Figure 3a). In addition to the microplankton (diatoms, dinoflagellates, and DDAs) (Figure 3a), nanoplankton like Cryptophytes, Prasinophytes and Haptophytes were also observed in large numbers in the two regions where DIN was available albeit at low concentrations (Figure 3b). This included the plume region and the mesohaline region where DDAs replenish DIN when cells disintegrate. Cryptophytes proliferated only in the low salinity plume waters with numbers ranging from 3.2×10^3 – 6.3×10^5 L⁻¹. This was also the case with prasinophytes but Haptophytes were seen in both the plume and the mesohaline area coincident with the DDA blooms (Figure 3b). Picoplanktonic *Synechococcus* (Figure 3c) were also seen in large numbers especially in the plume where their numbers ranged from 5.0×10^3 – 6.9×10^5 L⁻¹. Outside of the plume, *Synechococcus* were only seen in the mesohaline, DDA dominated region. Conversely, *Prochlorococcus* identified by their unique Divinyl Chl *a* signature were absent from the nutrient rich plume waters but were ubiquitous elsewhere especially in the waters east of the plume (Figure 3b), where all three macro nutrients were below the level of detection.

The significance of the ARP in driving changes in the hydrography, chemistry, and phytoplankton communities of the western Tropical North Atlantic is illustrated by

Principal Component Analysis (PCA) of hydrographic data and microscopic and CHEMTAX derived phytoplankton communities (Figure 4a). PCA enables a visualization of the similarities and differences between samples, as well as the correlations between the variables. The first principle component accounted for 32% of the variance and divided the data set into phytoplankton communities that proliferated in the plume (diatoms, dinoflagellates, cryptophytes and prasinophytes) from those in the mesohaline and oligotrophic waters (DDAs, *Trichodesmium*, *Prochlorococcus*, and Haptophytes). The former group correlated with DIN indicating its importance in the growth of these micro and nanoplankton. The latter group which comprised diazotrophs, Haptophytes, and picoplanktonic *Prochlorococcus* with low nutrient requirements were found in high salinity waters outside of the plume. The PC2 axis separated DIN, the limiting nutrient from DIP and silicate which were not limiting.

ECS

Our four-year study clearly demonstrated that the hydrochemical environment of the ECS undergoes large interannual variations linked to the discharge of the Changjiang River and the eastward movement of its plume (CDW) which strongly influences phytoplankton distribution. As in the case of the ARP, and based on T-S plots, Xu et al. (2018) defined three water types viz. CDW ($T > 23^\circ\text{C}$, $S < 28$) primarily influenced by discharge from the Changjiang River, the Kuroshio surface waters associated with the deeper, higher salinity Kuroshio waters ($S > 32.9$) and the Shelf waters. The latter is a mixed water mass (Salinity of 30–32.9) of the CDW and Kuroshio surface waters, located in the central part (125–128°E) of our study area. The large interannual variability in temperature, salinity and nutrients of the ECS was mainly from the variable influence of CDW and Kuroshio surface waters as is evident in Figures 5a–v. The influence of the CDW was greatest in 2010 with colder, lower salinity waters extending up to 127.5°E (Figures 5b,f) followed by the consecutive year of 2011 when the CDW was confined to west of 126°E (Figures 5c,g). In contrast, 2009 and 2013 experienced a greater influence of warmer, more saline Kuroshio surface

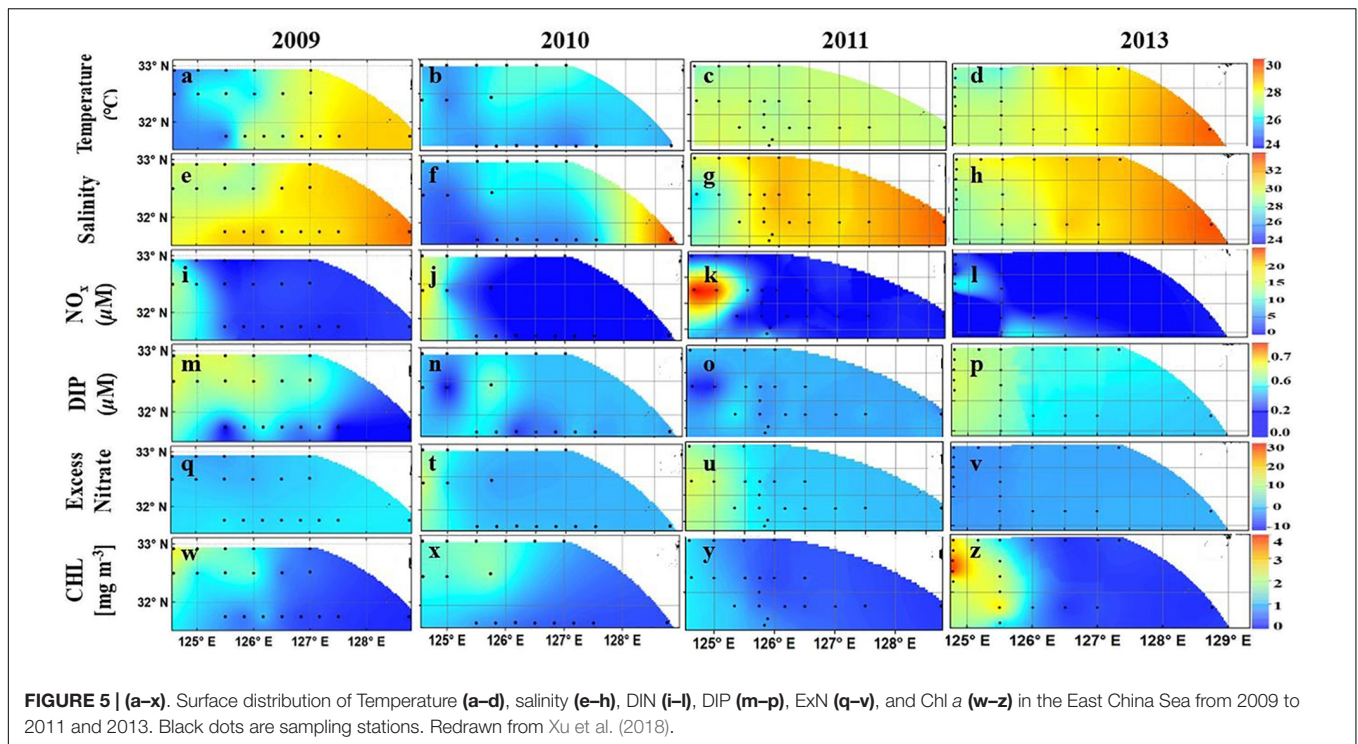


waters (Figures 5a,e,d,h). This resulted in mixed Shelf waters covering the entire study area. During these 2 years, waters in the eastern part of the observation area were warmer (SST > 28.5°C) (Figures 5a,d) and more saline (> 32.9) (Figures 5e,h).

The surface waters of the eastern region of the study area, which are less influenced by riverine discharge and in the path of the Kuroshio extension were generally depleted of nutrients during all 4 years of study. DIN in these waters ranged from 0.02 to 0.11 μM (Figures 5i-l), and DIP was less than 0.07 μM (Figures 5m-p). In these Kuroshio influenced waters, ExN measured around 0 μM (Figures 5q-v) indicating invariant stoichiometry. In contrast, the CDW waters showed distinct interannual differences in their nutrient regime with significantly higher (non-parametric Mann-Whitney U test, $p < 0.05$) ExN values in 2010 and 2011 (5–25 μM) (Figures 5t,u) indicating severe DIP limitation. This is contrast to 2009 and 2013 when ExN was < 0 μM (Figures 5q,v). As expected, in the former years, the CDW was characterized by extremely high DIN (> 10 μM , maximum of 26.1 μM) derived from the anthropogenic load of the Changjiang River (Figures 5j,k) but low DIP (< 0.05 μM) (Figures 5n,o). A contrasting situation emerged in 2009 and 2013 when only one station to the west of 125°E showed high DIN (Figures 5i,l). DIP in 2009 and 2013 was higher (up to 0.2 mg m^{-3}) compared to concentrations in 2010 and 2011 when it was almost below the limit of detection. Statistically, the differences in DIN, DIP, and ExN between higher DIP years (2009, 2013) and high lower DIP years (2010, 2011) were highly significant ($p < 0.01$) indicating the predominant influence of the Changjiang River on the stoichiometry of the ECS. Overall, phytoplankton biomass reflected the large west-east differences

in N:P ratios in the ECS. Chl *a* was higher in the CDW region (0.25–4.0 mg m^{-3}) but decreased in the shelf waters (0.14–0.9 mg m^{-3}) (Figures 5w-z). Lowest values were observed in Kuroshio surface waters where Chl *a* rarely exceeded 0.2 mg m^{-3} .

Similar to phytoplankton communities in the ARP continuum, those in the ECS also adapted to the changing nutrient regime influenced by the Changjiang River discharge. Phytoplankton communities of the CDW (Figure 6) showed clear distinctions between low DIP (2010, 2011) and high DIP (2009, 2013) years. Diatoms dominated the latter years and diatom-derived Chl *a* ranged from 3–2.1 mg m^{-3} compared to concentrations of 0.02–0.34 mg m^{-3} during low DIP years. In contrast, during 2010 and 2011, cyanobacteria dominated, contributing 6–76% of the Chl *a* as opposed to 1–20% in 2009 and 2013. A substantial population of Prymnesiophytes also contributed to the Chl *a* (25–55%) in 2013. Although we have chosen to show only the phytoplankton community structure of the CDW, it is apparent from Figure 4b of Xu et al. (2018) that there were no interannual differences in the phytoplankton structure of the mixed shelf waters. However, diatom populations did show dominance in the high DIP year of 2009 (Chl *a* contribution 28–83%). A mixture of cyanobacteria and the picoplanktonic prochlorophytes dominated (> 61% of the total Chl *a*) the low Chl *a* at waters of the oligotrophic Kuroshio surface waters during all 4 years of study (Figure 4c in Xu et al., 2018). Prochlorophytes, the second highest group after cyanobacteria, comprised more than 30% of the phytoplankton community in 2009, 2010, and 2013 and 19% in 2011 (Xu et al., 2018). Diatoms were



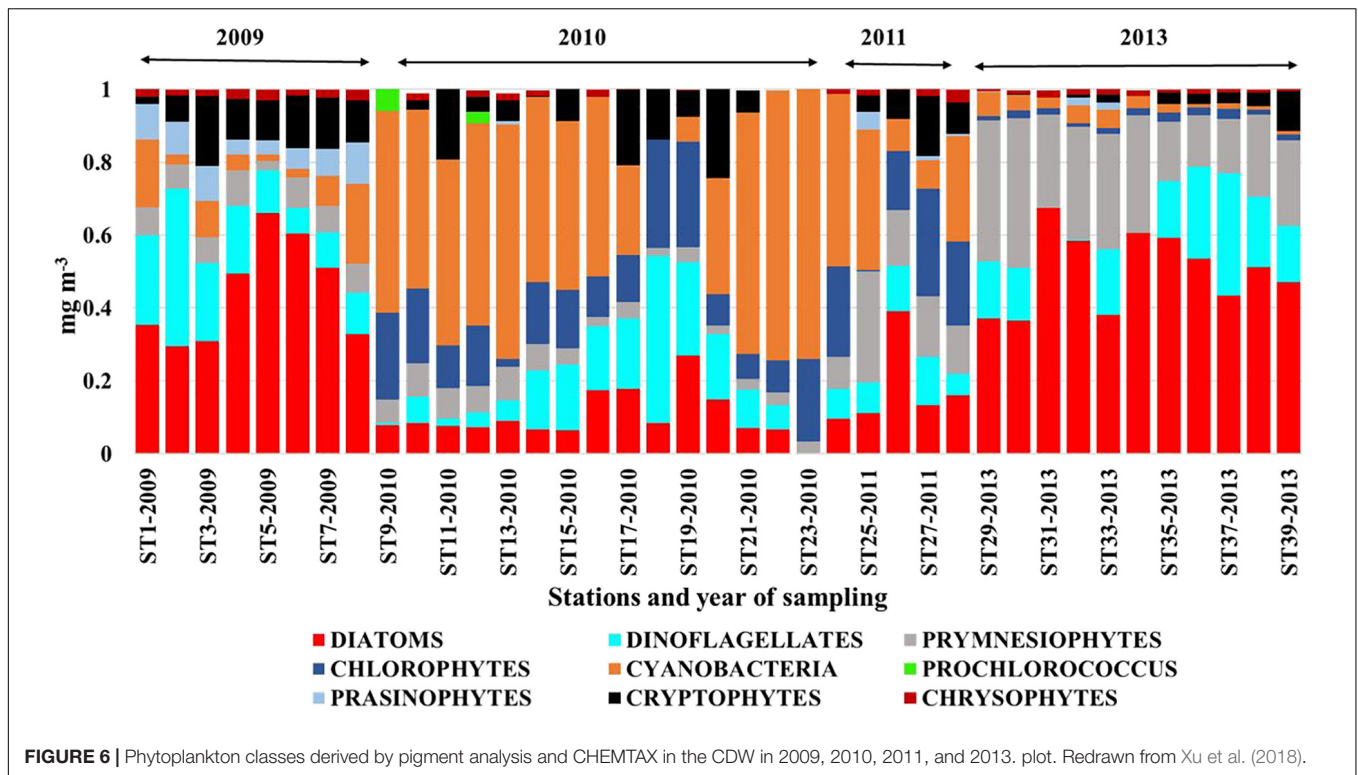
absent or negligible except in 2011 when 18% of Chl *a* was from this group. As in the case of the ARP (Goes et al., 2014), large diatom blooms were seen in the coastal waters of the Changjiang River Continuum (Zhou et al., 2008; Guo et al., 2014) advantaged by the abundant nutrients available from the river discharge.

The possible dependence of the various algal groups on Salinity, Temperature and nutrients is also examined by means of PCA (Figure 4b). PC1 accounted for 27.3% of the variance in this data separating DIP and DIN. PC1 also divided the data set into large microplankton (diatoms and dinoflagellates) with high P requirements versus smaller nano and picoplankton such as Chlorophytes, Cyanobacteria and Prochlorophytes which can grow at lower DIP concentrations. DIP correlated with large microplankton (diatoms and dinoflagellates) showing it to be the limiting nutrient that determined the transition from small to large phytoplankton in the CDW. Conversely, cyanobacteria, chlorophytes, and prochlorophytes were associated with warmer waters of low DIP concentrations characteristic of Kuroshio surface waters. This is also demonstrated by the positive correlation of smaller phytoplankton with ExN on PCA1 axis and the converse with microplankton. Both PC1 and PC2 show a strong negative correlation between Salinity and DIN indicating riverine inputs of DIN. In contrast to PC1, the PC2 axis which accounted for 24% of the variance in the dataset showed a positive correlation between DIN, DIP, and diatoms but notably a negative correlation with Temperature. This typifies the intrusion of colder, upwelled waters which bring in DIP and result in the domination of diatoms. The latter is elaborated further in the Discussion section.

DISCUSSION

Revisiting and comparing the previously conducted research in two of the world's largest river-ocean systems gave us an opportunity to understand how fluctuations in nutrient availability and nutrient ratios shape phytoplankton communities along the river-ocean continuum to produce highly distinct and specialized groups that can profoundly affect the food web and carbon fluxes to deeper depths. As we discuss below, it is likely that the N:P supply ratios from the two systems determine whether or not diazotrophs are part of the community, while it is likely that supply of a single limiting nutrient (such as DIP) is responsible for the interannual variability seen in the ECS. We use resource competition theory and resource supply ratio to describe the distribution of phytoplankton communities of the ARP and CDW in relation to changing in N:P supply ratios and changing DIP supplies along the river-ocean continuums.

Simply stated, Tilman (1977)'s resource competition theory states that in an equilibrium environment, each competing phytoplankton type is capable of drawing the limiting nutrient down to distinct low subsistence concentrations, known as R^* . The value of R^* for any nutrient is set by the ecophysiological characteristics of the phytoplankton type and represents both the concentration of the limiting nutrient at which growth is balanced by mortality (top down) and the minimum nutrient concentration (bottom up) required for survival (Ward et al., 2014). If multiple organism types are present, the ambient resource concentration will be drawn down to the lowest R^* and only that class of organisms will survive while other organisms will be excluded over time (Dutkiewicz et al., 2009). This theory then implies that the smallest cells which have higher



nutrient uptake rates should accumulate biomass by drawing down nutrients to the lowest level thus excluding any larger phytoplankton with higher nutrient requirements. However, this is not the case because the smallest and most competitive phytoplankton groups are in fact kept under control by grazing by the small zooplankton, allowing larger size classes to become established when excess nutrients become available (Ward et al., 2012; Ward et al., 2014). In this situations the R*s intersect and stable coexistence is possible. Thus, when nutrient supplies are higher, more classes of larger phytoplankton (with less efficient nutrient uptake rates) could coexist with the smallest types. This seems to be the case in the ECS where the CDW waters were DIP limited. However, in years (2009, 2013) when DIP concentrations increased we saw predominance of diatoms while in years when DIP concentrations were low or beyond the level of detection, small cells like cyanobacteria and chlorophytes predominated. Dinoflagellates remained invariant during all 4 years of sampling with Chl *a* ranging from 0.1–0.4 mg m⁻³ of the total Chl *a*. Many dinoflagellates are mixotrophic, and it is possible that this mixing of trophic levels allows them to exist in all situations.

On the eastern side of our sampling grid, in the oligotrophic waters dominated by the nutrient poor Kuroshio surface waters only picoplanktonic *Prochlorococcus* proliferated (Xu et al., 2018). The increased DIP concentrations appear to be regulated by the extent of low saline CDW in the western region which as determined by the surface temperature and salinity was limited westward in 2009 and 2013. In our more extensive study (Xu et al., 2018), we have investigated the physical forces driving the higher DIP concentrations in the mid-shelf of the ECS in 2009

and 2013. All evidence points to upwelling of DIP-rich Kuroshio Intermediate Water onto the upper layers of the shelf (Tseng et al., 2014) and its advection eastward by the CDW into the mid-shelf of the ECS. In Xu et al. (2018) we explain the higher surface DIP in 2009 and 2013 and the converse situation in 2010 and 2011 as follows. In the latter, when the Changjiang River discharge was higher, DIP from coastal upwelling was not only diluted as the CDW moved eastward, vertical stratification from density differences also prevented mixing. In contrast, during low discharge years, DIP from coastal upwelling could be transported further eastward into the mid-shelf where it supported the growth of larger phytoplankton.

In case of the ARP, we can also explain the appearance of diazotrophs versus non-diazotrophs (non-nitrogen fixing marine phytoplankton) in terms of the resource supply-ratio theory. Ward et al. (2013) describes the competition between the two (diazotrophs versus non-diazotrophs) through their interaction with the three essential nutrient elements *viz.* Fe, DIN and DIP. Fe is not limiting for phytoplankton both in the ARP and the CDW largely because of intense weathering and erosion that takes place in the drainage basins of this river system (Edmond et al., 1985; Bergquist and Boyle, 2006). Whereas in the CDW, DIP appears to be the single nutrient that controls the size structure of phytoplankton communities, in the ARP, it is the N: P ratio that will determine whether diazotrophs or non-diazotrophs will establish themselves. Generally, diazotrophs exhibit slower growth rates than non-diazotrophs so they will be outcompeted if both nutrients are limited. But if there is excess DIP relative to the stoichiometric requirements of the non-diazotrophs then this DIP can fuel diazotroph growth,

since it is assumed that diazotrophs can fix N. In other words, in situations where DIP:DIN supply rates are in excess of the non-diazotroph requirements, then diazotrophs can co-exist with the non-diazotrophs (Dutkiewicz et al., 2012). In the case of the ARP, away from the inner shelf where sediment load is reduced and light levels are not limiting, large mixed blooms (Shipe et al., 2006; Goes et al., 2014) deplete the DIN and reduce DIP although the riverine Si required for diatoms was not limiting. As the plume flows offshore, DIP is replenished through desorption (Fox et al., 1986; Berner and Rao, 1994) and the system transitions to diazotrophy and the acute shortage of DIN is thus mitigated. As stated earlier, a variety of diatom diazotroph assemblages as well as non-symbiotic and non-siliceous diazotrophs like *Trichodesmium* proliferated in the mesohaline waters. Small nitrogenous inputs from symbiotic diatoms supported populations of nanoplankton such as Prasinophytes and Haptophytes which were earlier not reported but are identified in this study using pigment biomarkers. Experimental evidence from other locations (Gulf of California and the subtropical North Pacific) shows that *Richelia* fixes 81–744% more N than needed for its own growth and up to 97.3% of the fixed N is transferred to the diatom partners (Foster et al., 2011). This same study also showed that N₂ fixation rates of *Richelia* and another cyanobacterial symbiont *Calothrix* were 171–420 times higher when the cells were symbiotic compared with the rates for the cells living freely.

It is well known that diazotrophy is inhibited when DIN and/or ammonium concentrations exceed 1 μM (Knapp, 2012) and the resource supply-ratio theory suggests that high N:P supply ratios will not support diazotrophy, so it is not surprising that we did not see either DDAs or non-symbiotic diazotrophs such as *Trichodesmium* in the ECS during our 4 years of study as DIN was not a limiting nutrient in these waters. What is noteworthy about the results from the ECS is the marked interannual variability in the hydrology, stoichiometry and consequent phytoplankton community structure of ECS modulated by the extent of the Changjiang River and its DIP inputs.

Long term changes being monitored in the ECS using satellite-derived salinity algorithms (Bai et al., 2014) show that the spread and direction of CDW plume on the ECS continental shelf are affected by the Changjiang River discharge while other long term studies of summer phytoplankton community in the Changjiang estuary during the past 50 years (Jiang et al., 2014) suggest that anthropogenic loading is leading to increase in smaller phytoplankton and dinoflagellates which could exacerbate harmful algal blooms. Although similar information is not available for the Amazon River continuum, model projections of climate change effects on discharge and inundation in the Amazon basin (Sorribas et al., 2016) show a system in transition (Davidson et al., 2012). A study of all the rivers of South America (van der Struijk and Kroeze, 2010) including the Amazon river shows that exports of DIN and DIP increased between 1970 and 2000 although the increases were more prominent in rivers south of the Amazon. If DIN export were to increase and attain concentrations higher than DIP loading, then we would expect

diazotrophy to disappear from the ARP. Elsewhere, nutrient reduction measures such as in the Chesapeake Bay Estuary along the east coast of the US, have resulted in a decrease in diatoms from a decrease in DIN (Harding et al., 2015) whereas the reverse was seen in Patos Lagoon Estuary, Brazil which showed increasing signs of eutrophication (Haraguchi et al., 2015). Not surprisingly and considering the extent of the rapid economic development of China during the past 30 years, the Pearl River which empties into the northern part of South China Sea showed the same situation that we observed in the ECS. While diatoms proliferated in the inner estuary, limited DIP resulted in the proliferation of picophytoplankton in the mesohaline and nearshore oceanic waters (Qiu et al., 2010).

The varied taxonomical diversity of the two river continuums should be reflected in the geochemical fluxes to deeper depth. Variations in the impact of the CDW through its nutrient supply and consequently on the phytoplankton community are also reflected in the carbon fluxes. Sukigara et al. (2017) who operated sediment traps in 2000 and 2011 in tandem with our studies, showed that sinking particles were thrice as high in 2000 when our study showed the dominance of diatoms than in 2011. Particulate carbon and nitrogen contents as well as isotope ratios, showed that the particles that sunk out the euphotic zone in 2010 were primarily from the CDW layer with a secondary contribution from the SCM layer. Concomitant with our ARP studies Chong et al. (2014), showed a distinct axis of POC and biogenic silica deposition on the deep floor aligned with the plume and a footprint of approximately 1 million km² of carbon and biogenic silica on the deep sea floor.

Traditionally, the elemental stoichiometry of both phytoplankton biomass and dissolved nutrient pools has been viewed as having limited variability. Expressing the relevance of the canonical Redfield ratio, Falkowski and Davis (2004) wrote that “the uniformity of elemental Redfield ratios in the oceans and the life they contain underpins our understanding of marine biogeochemistry.” But just as this near-constant ratio laid the foundations for the twentieth-century advances in our understanding of marine biogeochemistry, deviations from this ratio are now providing twenty-first-century insights into the nutrient dynamics of oceans modern and ancient (Nature Geoscience, 2014). Questions remain with respect to fundamental facts such as the flexibility of phytoplankton stoichiometry and the relationship of internal ratios to resource availability and growth rates (Hillebrand et al., 2013). Relationship between available and internal N:P ratios are not necessarily linear. While Goldman et al. (1979) found that phytoplankton N:P ratios varied widely at low N:P converging to classic N:P ratio of 16 only at high growth rates, Hillebrand et al. (2013) revisited this premise to show that although N:P ratios did converge to an optimal ratio it was different for different species and phylogenetic groups. We think that river continuums with changing spatial and temporal stoichiometry are ideal environments to study the flexibility of phytoplankton stoichiometry *vis a vis* resource availability and its implications for size and functional traits.

CONCLUSION

We have compared the distribution of phytoplankton communities in the river-ocean continuums of two of the world's largest rivers, the Amazon River, the nutrient content of which is largely governed by forest derived nutrients and the Changjiang River, the waters of which are heavily impacted by human activities. We show that phytoplankton communities along the axes of their plumes are shaped largely by the initial N: P content of the rivers. In the case of the ARP, phytoplankton populations downstream of the river plume were largely controlled by the availability of inorganic nitrogenous nutrients with diatoms dominating upstream where nitrogenous were available either from the source water or from the onshore advection of nutrient rich waters from depth. In the case of the Changjiang River plume, phytoplankton communities were limited significantly by a single nutrient *viz.* inorganic phosphate and downstream of the plume, diatoms were observed during years when coastal upwelling was more intense and inorganic phosphate from deeper depths advected offshore. One of the largest differences between the ARP and the Changjiang River plume waters was the absence of DDAs and *Trichodesmium* spp. in the latter, which appears to be tied to different N:P supply ratios.

AUTHOR CONTRIBUTIONS

HG wrote the paper and conducted the Amazon plume research. QX conducted the East China Sea research. JG conducted research in the Amazon plume. EC undertook the cell counts for

the Amazon plume research. JI and PY were the lead PIs on the East China Sea and Amazon Plume projects respectively.

FUNDING

This work was supported by Visiting Professorships at Nagoya University, Japan to HG and JG. Research conducted in the ECS by JI and QX was supported by JAXA GCOM-C and JSPS KAKENHI grant number JP26241009 awarded to JI. Research work in the ARP was supported by grants NSF OCE-0934095 and 1133277 to PY, JG, and HG and NASA grants NNX13AI29A and NNX16AD40G to JG and HG.

ACKNOWLEDGMENTS

We are highly indebted to Dr. Simon Wright (Australian Antarctic Division) for the CHEMTAX code and for his constant help and guidance in running CHEMTAX. We would specially like to thank Dr. Stephanie Dutkiewicz (MIT) for her time, effort and invaluable suggestions that improved this paper immensely. We thank the NASA-HPLC Center, for help with analysis of phytoplankton pigments for the ARP study. We thank Victoria Coles (Center for Environmental Science, University of Maryland) for the Salinity distribution map of the ARP and we acknowledge the Salinity map for the ECS provided by Asia-Pacific Data Research Center.

REFERENCES

- Anderson, D. M., Glibert, P. M., and Burkholder, J. M. (2002). Harmful algal blooms and eutrophication: nutrient sources, composition, and consequences. *Estuaries* 25, 704–726. doi: 10.1007/BF02804901
- Armbrecht, L. H., Wright, S. W., Petocz, P., and Armand, L. K. (2015). A new approach to testing the agreement of two phytoplankton quantification techniques: microscopy and CHEMTAX. *Limnol. Oceanogr.* 13, 425–437. doi: 10.1002/lom3.10037
- Bai, Y., He, X., Pan, D., Chen, C.-T. A., Kang, Y., Chen, X., et al. (2014). Summertime Changjiang River plume variation during 1998–2010. *J. Geophys. Res.* 119, 6238–6257. doi: 10.1002/2014JC009866
- Barlow, R., Gibberd, M. J., Lamont, T., Aiken, J., and Holligan, P. (2016). Chemotaxonomic phytoplankton patterns on the eastern boundary of the Atlantic Ocean. *Deep Sea Res. Part I* 111, 73–78. doi: 10.1016/j.dsr.2016.02.011
- Bergquist, B. A., and Boyle, E. A. (2006). Iron isotopes in the Amazon River system: weathering and transport signatures. *Earth Planet. Sci. Lett.* 248, 54–68. doi: 10.1016/j.epsl.2006.05.004
- Berner, R. A., and Rao, J.-L. (1994). Phosphorus in sediments of the Amazon River and estuary: implications for the global flux of phosphorus to the sea. *Geochim. Cosmochim. Acta* 58, 2333–2339. doi: 10.1016/0016-7037(94)90014-0
- Beusen, A. H. W., Bouwman, A. F., Van Beek, L. P. H., Mogollón, J. M., and Middelburg, J. J. (2016). Global riverine N and P transport to ocean increased during the 20th century despite increased retention along the aquatic continuum. *Biogeosciences* 13, 2441–2451. doi: 10.5194/bg-13-2441-2016
- Bouwman, A. F., Van Drecht, G., Knoop, J. M., Beusen, A. H. W., and Meinardi, C. R. (2005). Exploring changes in river nitrogen export to the world's oceans. *Global Biogeochem. Cycles* 19:GB1002. doi: 10.1029/2004GB002314
- Carpenter, E. J., Montoya, J. P., Burns, J., Mulholland, M. R., Subramaniam, A., and Capone, D. G. (1999). Extensive bloom of a N₂-fixing diatom/cyanobacterial association in the tropical Atlantic Ocean. *Mar. Ecol. Prog. Ser.* 185, 273–283. doi: 10.3354/meps185273
- Chen, C. T. (2008). Distributions of nutrients in the East China Sea and the South China Sea connection. *J. Oceanogr.* 64, 737–751. doi: 10.1007/s10872-008-0062-9
- Chen, C. T., and Wang, S. L. (1999). Carbon, alkalinity and nutrient budgets on the East China Sea continental shelf. *J. Geophys. Res.* 104, 20675–20686. doi: 10.1029/1999JC900055
- Chisholm, S. W., Frankel, S. L., Goericke, R., Olson, R. J., Palenik, B., Waterbury, J. B., et al. (1992). *Prochlorococcus marinus* nov. gen. nov. sp.: an oxyphototrophic marine prokaryote containing divinyl chlorophyll a and b. *Arch. Microbiol.* 157, 297–300. doi: 10.1007/BF00245165
- Chong, L. S., Berelson, W. M., Mcmanus, J., Hammond, D. E., Rollins, N. E., and Yager, P. L. (2014). Carbon and biogenic silica export influenced by the Amazon River Plume: patterns of remineralization in deep-sea sediments. *Deep Sea Res. I* 85, 124–137. doi: 10.1016/j.dsr.2013.12.007
- Coles, V. J., Brooks, M. T., Hopkins, J., Stukel, M. R., Yager, P. L., and Hood, R. R. (2013). The pathways and properties of the Amazon River Plume in the tropical North Atlantic Ocean. *J. Geophys. Res.* 118, 6894–6913. doi: 10.1002/2013JC008981
- Conroy, B. J., Steinberg, D. K., Song, B., Kalmbach, A., Carpenter, E. J., and Foster, R. A. (2017). Mesozooplankton Graze on cyanobacteria in the Amazon river plume and western tropical north Atlantic. *Front. Microbiol.* 8:1436. doi: 10.3389/fmicb.2017.01436
- Conroy, B. J., Steinberg, D. K., Stukel, M. R., Goes, J. I., and Coles, V. J. (2016). Meso- and microzooplankton grazing in the Amazon River plume and western

- tropical North Atlantic. *Limnol. Oceanogr.* 61, 825–840. doi: 10.3389/fmicb.2017.01436
- Dandonneau, Y., and Niang, A. (2007). Assemblages of phytoplankton pigments along a shipping line through the North Atlantic and tropical Pacific. *Prog. Oceanogr.* 73, 127–144. doi: 10.1016/j.pocean.2007.02.003
- Davidson, E. A., de Araújo, A. C., Artaxo, P., Balch, J. K., Brown, I. F., C., Bustamante, M. M., et al. (2012). The Amazon basin in transition. *Nature* 481, 321–328. doi: 10.1038/nature10717
- Del Vecchio, R., and Subramaniam, A. (2004). Influence of the Amazon River on the surface optical properties of the western tropical North Atlantic Ocean. *J. Geophys. Res.* 109:C11001. doi: 10.1029/2004JC002503
- DeMaster, D. J. (1996). Biogeochemical processes in Amazon shelf waters: chemical distributions and uptake rates of silicon, carbon and nitrogen. *Continental Shelf Res.* 16, 617–643. doi: 10.1016/0278-4343(95)00048-8
- Dutkiewicz, S., Follows, M. J., and Bragg, J. G. (2009). Modeling the coupling of ocean ecology and biogeochemistry. *Global Biogeochem. Cycles* 23:GB4017. doi: 10.1029/2008GB003405
- Dutkiewicz, S., Ward, B. A., Monteiro, F., and Follows, M. J. (2012). Interconnection of nitrogen fixers and iron in the Pacific Ocean: theory and numerical simulations. *Global Biogeochem. Cycles* 26:GB1012. doi: 10.1029/2011GB004039
- Edmond, J. M., Spivack, A., Grant, B. C., Ming-Hui, H., Zexiam Chen, S., and Zeng Xiushou, C. (1985). Chemical dynamics of the Changjiang estuary. *Continental Shelf Res.* 4, 17–36. doi: 10.1016/0278-4343(85)90019-6
- Falkowski, P. G., and Davis, C. S. (2004). Natural proportions. *Nature* 431:131. doi: 10.1038/431131a
- Foster, R. A., Kuypers, M. M. M., Vagner, T., Paerl, R. W., Musat, N., and Zehr, J. P. (2011). Nitrogen fixation and transfer in open ocean diatom–cyanobacterial symbioses. *ISME J.* 5, 1484–1493. doi: 10.1038/ismej.2011.26
- Foster, R. A., Subramaniam, A., Mahaffey, C., Carpenter, E. J., Capone, D. G., and Zehr, J. P. (2007). Influence of the Amazon River plume on distributions of free-living and symbiotic cyanobacteria in the western tropical north Atlantic Ocean. *Limnol. Oceanogr.* 52, 517–532. doi: 10.4319/lo.2007.52.2.0517
- Fox, L. E., Sager, S. L., and Wofsy, S. C. (1986). The chemical control of soluble phosphorus in the Amazon estuary. *Geochim. Cosmochim. Acta* 50, 783–794. doi: 10.1016/0016-7037(86)90354-6
- Furuya, K., Hayashi, M., Yabushita, Y., and Ishikawa, A. (2003). Phytoplankton dynamics in the East China Sea in spring and summer as revealed by HPLC-derived pigment signatures. *Deep Sea Res. II* 50, 367–387. doi: 10.1016/S0967-0645(02)00460-5
- Glibert, P. M., Allen, J. I., Bouwman, A. F., Brown, C. W., Flynn, K. J., Lewitus, A. J., et al. (2010). Modeling of HABs and eutrophication: status, advances, challenges. *J. Mar. Syst.* 83, 262–275. doi: 10.1016/j.jmarsys.2010.05.004
- Glibert, P. M., Maranger, R., Sobota, D. J., and Bouwman, L. (2014). The Haber Bosch–harmful algal bloom (HB–HAB) link. *Environ. Res. Lett.* 9:105001. doi: 10.1088/1748-9326/9/10/105001
- Goes, J. I., Gomes, H. D. R., Chelkalyuk, A. M., Carpenter, E. J., Montoya, J. P., Coles, V. J., et al. (2014). Influence of the Amazon River discharge on the biogeography of phytoplankton communities in the western tropical north Atlantic. *Prog. Oceanogr.* 120, 29–40. doi: 10.1016/j.pocean.2013.07.010
- Goldman, J. C., Mccarthy, J. J., and Peavey, D. G. (1979). Growth rate influence on the chemical composition of phytoplankton in oceanic waters. *Nature* 279:210. doi: 10.1038/279210a0
- Guo, S., Feng, Y., Wang, L., Dai, M., Liu, Z., Bai, Y., et al. (2014). Seasonal variation in the phytoplankton community of a continental-shelf sea: the East China Sea. *Mar. Ecol. Progr. Ser.* 516, 103–126. doi: 10.3354/meps10952
- Haraguchi, L., Carstensen, J., Abreu, P. C., and Odebrecht, C. (2015). Long-term changes of the phytoplankton community and biomass in the subtropical shallow Patos Lagoon Estuary, Brazil. *Estuar. Coast. Shelf Sci.* 162, 76–87. doi: 10.1016/j.ecss.2015.03.007
- Harding, L. W., Adolf, J. E., Mallonee, M. E., Miller, W. D., Gallegos, C. L., Perry, E. S., et al. (2015). Climate effects on phytoplankton floral composition in Chesapeake Bay. *Estuar. Coast. Shelf Sci.* 162, 53–68. doi: 10.1038/srep23773
- Heisler, J., Glibert, P. M., Burkholder, J. M., Anderson, D. M., Cochlan, W., Dennison, W. C., et al. (2008). Eutrophication and harmful algal blooms: a scientific consensus. *Harmful Algae* 8, 3–13. doi: 10.1016/j.hal.2008.08.006
- Higgins, H. W., Wright, S. W., and Schlüter, L. (2011). *Quantitative Interpretation of Chemotaxonomic Pigment Data: Phytoplankton Pigments: Characterization, Chemotaxonomy and Applications in Oceanography*. London: Cambridge University Press.
- Hillebrand, H., Steinert, G., Boersma, M., Malzahn, A., Meunier, C. L., Plum, C., et al. (2013). Goldman revisited: faster-growing phytoplankton has lower N : P and lower stoichiometric flexibility. *Limnol. Oceanogr.* 58, 2076–2088. doi: 10.4319/lo.2013.58.6.2076
- Hooker, S. B., Heukelem, L. V., Thomas, C. S., Claustre, H., Ras, J., Barlow, R., et al. (2005). *The Second SeaWiFS HPLC Analysis Round Robin Experiment (SeaHARRE-2)*. Greenbelt, MD: NASA Goddard Space Flight Center.
- Hu, C., Montgomery, E. T., Schmitt, R. W., and Muller-Karger, F. E. (2004). The dispersal of the Amazon and Orinoco River water in the tropical Atlantic and Caribbean Sea: observation from space and S-PALACE floats. *Deep Sea Res. II* 51, 1151–1171. doi: 10.1016/S0967-0645(04)00105-5
- Jiang, Z., Liu, J., Chen, J., Chen, Q., Yan, X., Xuan, J., et al. (2014). Responses of summer phytoplankton community to drastic environmental changes in the Changjiang (Yangtze River) estuary during the past 50 years. *Water Res.* 54, 1–11. doi: 10.1016/j.watres.2014.01.032
- Jiao, N., Yang, Y., Hong, N., Ma, Y., Harada, S., Koshikawa, H., et al. (2005). Dynamics of autotrophic picoplankton and heterotrophic bacteria in the East China Sea. *Continental Shelf Res.* 25, 1265–1279. doi: 10.1016/j.csr.2005.01.002
- Jickells, T. D., Buitenhuis, E., Altieri, K., Baker, A. R., Capone, D., Duce, R. A., et al. (2017). A reevaluation of the magnitude and impacts of anthropogenic atmospheric nitrogen inputs on the ocean. *Global Biogeochem. Cycles* 31, 289–305. doi: 10.1002/2016GB005586
- Knapp, A. N. (2012). The sensitivity of marine N(2) fixation to dissolved inorganic nitrogen. *Front. Microbiol.* 3:374. doi: 10.3389/fmicb.2012.00374
- Latasa, M. (2007). Improving estimations of phytoplankton class abundances using CHEMTAX. *Mar. Ecol. Progr. Ser.* 329, 13–21. doi: 10.3354/meps329013
- Li, J., Glibert, P. M., Zhou, M., Lu, S., and Lu, D. (2009). Relationships between nitrogen and phosphorus forms and ratios and the development of dinoflagellate blooms in the East China Sea. *Mar. Ecol. Progr. Ser.* 383, 11–26. doi: 10.3354/meps07975
- Mackey, M. D., Dj, M., Hw, H., and Sw, W. (1996). CHEMTAX - a program for estimating class abundances from chemical markers: application to HPLC measurements of phytoplankton. *Mar. Ecol. Progr. Ser.* 144, 265–283. doi: 10.3354/meps144265
- Muller-Karger, F. E., McClain, C. R., and Richardson, P. L. (1988). The dispersal of the Amazon's water. *Nature* 333, 56–59. doi: 10.1038/333056a0
- Nature Geoscience (2014). Eighty years of Redfield. *Nat. Geosci.* 7:849.
- Qiu, D., Huang, L., Zhang, J., and Lin, S. (2010). Phytoplankton dynamics in and near the highly eutrophic Pearl River Estuary, South China Sea. *Continental Shelf Res.* 30, 177–186. doi: 10.1016/j.marpolbul.2011.01.018
- Seitzinger, S. P., Mayorga, E., Bouwman, A. F., Kroeze, C., Beusen, A. H. W., Billen, G., et al. (2010). Global river nutrient export: a scenario analysis of past and future trends. *Global Biogeochem. Cycles* 24:GB0A08. doi: 10.1016/j.scitotenv.2009.12.015
- Serive, B., Nicolau, E., Bérard, J.-B., Kaas, R., Pasquet, V., Picot, L., et al. (2017). Community analysis of pigment patterns from 37 microalgae strains reveals new carotenoids and porphyrins characteristic of distinct strains and taxonomic groups. *PLoS One* 12:e0171872. doi: 10.1371/journal.pone.0171872
- Sharples, J., Middelburg, J. J., Fennel, K., and Jickells, T. D. (2017). What proportion of riverine nutrients reaches the open ocean? *Global Biogeochem. Cycles* 31, 39–58. doi: 10.1002/2016GB005483
- Shipe, R. F., Curtaz, J., Subramaniam, A., Carpenter, E. J., and Capone, D. G. (2006). Diatom biomass and productivity in oceanic and plume-influenced waters of the western tropical Atlantic ocean. *Deep Sea Res. I* 53, 1320–1334. doi: 10.1016/j.dsr.2006.05.013
- Sorribas, M. V., Paiva, R. C. D., Melack, J. M., Bravo, J. M., Jones, C., Carvalho, L., et al. (2016). Projections of climate change effects on discharge and inundation in the Amazon basin. *Clim. Change* 136, 555–570. doi: 10.1007/s10584-016-1640-2
- Stukel, M. R., Coles, V. J., Brooks, M. T., and Hood, R. R. (2014). Top-down, bottom-up and physical controls on diatom-diazotroph assemblage growth in the Amazon River plume. *Biogeosciences* 11, 3259–3278. doi: 10.5194/bg-11-3259-2014

- Subramaniam, A., Yager, P. L., Carpenter, E. J., Mahaffey, C., Björkman, K., Cooley, S., et al. (2008). Amazon River enhances diazotrophy and carbon sequestration in the tropical North Atlantic Ocean. *Proc. Natl. Acad. Sci. U.S.A.* 105, 10460–10465. doi: 10.1073/pnas.0710279105
- Sukigara, C., Mino, Y., Tripathy, S. C., Ishizaka, J., and Matsuno, T. (2017). Impacts of the Changjiang diluted water on sinking processes of particulate organic matters in the East China Sea. *Continental Shelf Res.* 151, 84–93. doi: 10.1016/j.csr.2017.10.012
- Swan, C. M., Vogt, M., Gruber, N., and Laufkoetter, C. (2016). A global seasonal surface ocean climatology of phytoplankton types based on CHEMTAX analysis of HPLC pigments. *Deep Sea Res. I* 109, 137–156. doi: 10.1016/j.dsr.2015.12.002
- Tilman, D. (1977). Resource competition between plankton algae: an experimental and theoretical approach. *Ecology* 58, 338–348. doi: 10.2307/1935608
- Torrecilla, E., Stramski, D., Reynolds, R. A., Millán-Núñez, E., and Piera, J. (2011). Cluster analysis of hyperspectral optical data for discriminating phytoplankton pigment assemblages in the open ocean. *Remote Sens. Environ.* 115, 2578–2593. doi: 10.1016/j.rse.2011.05.014
- Tseng, Y. F., Lin, J., Dai, M., and Kao, S. J. (2014). Joint effect of freshwater plume and coastal upwelling on phytoplankton growth off the Changjiang River. *Biogeosciences* 11, 409–423. doi: 10.5194/bg-11-409-2014
- van der Struijk, L. F., and Kroeze, C. (2010). Future trends in nutrient export to the coastal waters of South America: implications for occurrence of eutrophication. *Global Biogeochem. Cycles* 24, doi: 10.1029/2009GB003572
- Van Heukelem, L., and Thomas, C. S. (2001). Computer-assisted high-performance liquid chromatography method development with applications to the isolation and analysis of phytoplankton pigments. *J. Chromatogr. A* 910, 31–49. doi: 10.1016/S0378-4347(00)00603-4
- Vidussi, F., Claustre, H., Manca, B., Luchetta, A., and Marty, J. C. (2001). Phytoplankton pigment distribution in relation to upper thermocline circulation in the eastern Mediterranean Sea during winter. *J. Geophys. Res.* 106, 939–959. doi: 10.1029/1999JC000308
- Wang, B., and Wang, X. (2007). Chemical hydrography of coastal upwelling in the East China Sea. *Chin. J. Oceanol. Limnol.* 25, 16–26. doi: 10.1007/s00343-007-0016-x
- Ward, B. A., Dutkiewicz, S., and Follows, M. J. (2014). Modelling spatial and temporal patterns in size-structured marine plankton communities: top-down and bottom-up controls. *J. Plank. Res.* 36, 31–47. doi: 10.1093/plankt/fbt097
- Ward, B. A., Dutkiewicz, S., Jahn, O., and Follows, M. J. (2012). A size-structured food-web model for the global ocean. *Limnol. Oceanogr.* 57, 1877–1891. doi: 10.4319/lo.2012.57.6.1877
- Ward, B. A., Dutkiewicz, S., Moore, C. M., and Follows, M. J. (2013). Iron, phosphorus, and nitrogen supply ratios define the biogeography of nitrogen fixation. *Limnol. Oceanogr.* 58, 2059–2075. doi: 10.4319/lo.2013.58.6.2059
- Weber, S. C., Carpenter, E. J., Coles, V. J., Yager, P. L., Goes, J., and Montoya, J. P. (2017). Amazon River influence on nitrogen fixation and export production in the western tropical North Atlantic. *Limnol. Oceanogr.* 62, 618–631. doi: 10.1002/lno.10448
- Wolf, C., Frickenhaus, S., Kiliyas, E. S., Peeken, I., and Metfies, K. (2014). Protist community composition in the Pacific sector of the Southern Ocean during austral summer 2010. *Polar Biol.* 37, 375–389. doi: 10.1007/s00300-013-1438-x
- Wong, G. T. F., Gong, G. C., Liu, K. K., and Pai, S. C. (1998). ‘Excess Nitrate’ in the East China Sea. *Estuar. Coast. Shelf Sci.* 46, 411–418. doi: 10.1006/ecss.1997.0287
- Wood, F. E. J. (1966). A Phytoplankton Study of the Amazon Region. *Bull. Mar. Sci.* 16, 102–123.
- Wright, S., and Jeffrey, S. W. (2006). “Pigment markers for phytoplankton production,” in *Marine Organic Matter: Biomarkers, Isotopes and DNA*, ed. J. Volkman (Berlin: Springer), 71–104. doi: 10.1007/698_2_003
- Wright, S. W. (2005). *Analysis of Phytoplankton Populations using Pigment Markers. Course Notes for a Workshop Pigment Analysis of Antarctic Microorganisms*. Kuala Lumpur: University of Malaya,
- Xu, Q., Sukigara, C., Goes, J. I., Do Rosario Gomes, H., Zhu, Y., Wang, S., et al. (2018). Interannual changes in summer phytoplankton community composition in relation to water mass variability in the East China Sea. *J. Oceanogr.* 322, 31–47. doi: 10.1007/s10872-018-0484-y
- Yan, W., Mayorga, E., Li, X., Seitzinger, S. P., and Bouwman, A. F. (2010). Increasing anthropogenic nitrogen inputs and riverine DIN exports from the Changjiang River basin under changing human pressures. *Global Biogeochem. Cycles* 24:GB0A06. doi: 10.1029/2009GB003575
- Yang, D., Yin, B., Liu, Z., Bai, T., Qi, J., and Chen, H. (2012). Numerical study on the pattern and origins of Kuroshio branches in the bottom water of southern East China Sea in summer. *J. Geophys. Res.* 117:C05015. doi: 10.1029/2011JC007528
- Yang, D., Yin, B., Sun, J., and Zhang, Y. (2013). Numerical study on the origins and the forcing mechanism of the phosphate in upwelling areas off the coast of Zhejiang province, China in summer. *J. Mar. Syst.* 12, 1–18. doi: 10.1016/j.jmarsys.2013.04.002
- Zhang, J., Liu, S. M., Ren, J. L., Wu, Y., and Zhang, G. L. (2007). Nutrient gradients from the eutrophic Changjiang (Yangtze River) Estuary to the oligotrophic Kuroshio waters and re-evaluation of budgets for the East China Sea Shelf. *Progr. Oceanogr.* 74, 449–478. doi: 10.1016/j.pocean.2007.04.019
- Zhou, M.-J., Shen, Z.-L., and Yu, R.-C. (2008). Responses of a coastal phytoplankton community to increased nutrient input from the Changjiang (Yangtze) River. *Continental Shelf Res.* 28, 1483–1489. doi: 10.1016/j.csr.2007.02.009

Conflict of Interest Statement: The authors declare that the research was conducted in the absence of any commercial or financial relationships that could be construed as a potential conflict of interest.

Copyright © 2018 Gomes, Xu, Ishizaka, Carpenter, Yager and Goes. This is an open-access article distributed under the terms of the Creative Commons Attribution License (CC BY). The use, distribution or reproduction in other forums is permitted, provided the original author(s) and the copyright owner(s) are credited and that the original publication in this journal is cited, in accordance with accepted academic practice. No use, distribution or reproduction is permitted which does not comply with these terms.